

# Controlling spontaneous emission via electronic correlations in transparent metals

M. B. Silva Neto<sup>1</sup> and F. A. Pinheiro<sup>1</sup>

<sup>1</sup>*Instituto de Física, Universidade Federal do Rio de Janeiro, Caixa Postal 68528, Rio de Janeiro, Brazil*

We study the spontaneous emission of agglomerates of two-level quantum emitters embedded in a correlated transparent metal. The characteristic emission energy corresponds to the splitting between ground and excited states of a neutral, nonmagnetic molecular impurity (F color center), while correlations are due to the existence of narrow bands in the metal. This is the case of transition metal oxides with an  $ABO_3$  Perovskite structure, such as  $SrVO_3$  and  $CaVO_3$ , where oxygen vacancies are responsible for the emission of visible light, while the correlated metallic nature arises from the partial filling of a band with mostly  $d$ -orbital character. For these systems we put forward an interdisciplinary, tunable mechanism to control light emission governed by electronic correlations. We show that not only there exists a critical value for the correlation strength above which the metal becomes transparent in the visible, but also that strong correlations can lead to a remarkable enhancement of the light-matter coupling. By unveiling the role of electronic correlations in spontaneous emission, our findings set the basis for the design of controllable, solid-state, single-photon sources in correlated transparent metals.

Progresses in the understanding of light-matter interactions have enabled new mechanisms of controlling light emission, propagation and extraction on chip [1, 2]. Since the pioneering work of Purcell it has been known that spontaneous emission is not only determined by the emitters' (atoms, molecules, and quantum dots) intrinsic electronic levels but is also influenced by the surrounding electromagnetic environment [3]. This discovery has paved the way to the development of several different strategies to modify and tailor the spontaneous emission of quantum emitters, typically relying on different choices of material platforms and/or physical mechanisms that affect spontaneous emission. Photonic crystals [4], dielectric microcavities [5], nanophotonic waveguides [6], graphene-based structures [7, 8], dielectric [9] and plasmonic [10, 11] nanoantennas, and metamaterials [12–14] are examples of different material platforms that have been explored to that purpose. In particular, metamaterials and 2D metasurfaces are versatile systems to achieving far-field emission patterns with desired properties, such as divergence and directionality [15], and even completely suppressing light emission [16]. Metallic structures have also been employed to modify spontaneous emission, with plasmonic resonances being designed to increase the electric field and enhance the local density of states at the emitters location [17, 18]. Regarding the different physical mechanisms to modify light emission one may cite the Fano effect [19, 20] and critical phenomena. Indeed there are evidences, both theoretical [21–23] and experimental [24], that phase transitions affect spontaneous emission in a crucial way, thus allowing for the optical determination of critical exponents via the Purcell factor [25]. Altogether these different routes have allowed for many technological applications, such as solar cells [27], molecular imaging [26, 28], and single-photon sources [29].

In the present letter we propose a twofold, interdisciplinary strategy to control spontaneous emission that combines: i) an alternative material platform, transition metal oxides; and ii) a novel physical mechanism, electronic correlations. More specifically, we consider color center agglomerates incorporated into a correlated transparent metal, namely  $ABO_3$  Perovskites, such as  $SrVO_3$  and  $CaVO_3$ , where oxygen vacan-

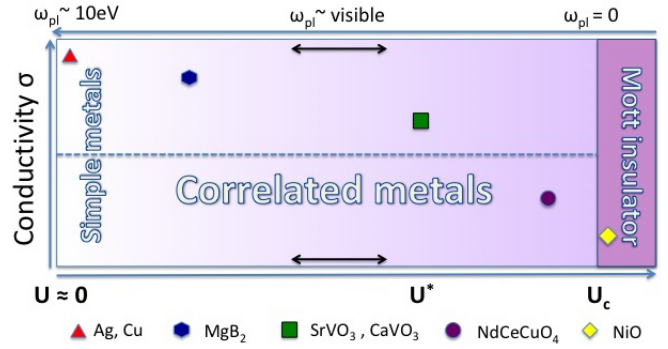


Figure 1. Schematic evolution of the conductivity,  $\sigma$ , and plasmon frequency,  $\omega_{pl}$ , as a function of the correlation strength,  $U$ . While simple metals like Ag and Cu are excellent conductors (large  $\sigma$ ) and highly reflective (large  $\omega_{pl}$ ), correlated metals such as  $SrVO_3$  and  $CaVO_3$  exhibit conductivities that are still higher than the best doped semiconductors (dashed line) while transmitting visible light very effectively as they have  $\omega_{pl}$  below the visible transparency window.

cies are responsible for emission of visible light [30] and electronic correlations arise from the narrowness of the partially filled B- ion,  $d$ -bands. Our choice for this particular material platform is motivated by the fact that transition metal oxides exhibit unique electrical and optical properties, such as excellent carrier mobilities, mechanical stress tolerance, compatibility with organic dielectric and photoactive materials, and high optical transparency [31]. These materials are also versatile and cost-effective to many applications in optoelectronics, such as electronic circuits, flexible organic light-emitting diode (OLED) displays, and solar cells [31].

A key issue while engineering metallic materials for optoelectronic applications relies on an adequate combination of high optical transparency and high electrical conductivity. This is usually challenging since the plasmon frequency of the best conducting metals is typically of the order of  $\hbar\omega_{pl} \sim 10\text{eV}$ , well above the visible transparency window  $1.8\text{eV} \leq \hbar\omega \leq 3.1\text{eV}$ , see Fig. 1. Hence achieving transparency in good conductors requires minimizing the plasmon frequency  $\omega_{pl}^2 = e^2 n / \epsilon_0 m^*$  (given in terms of the electric

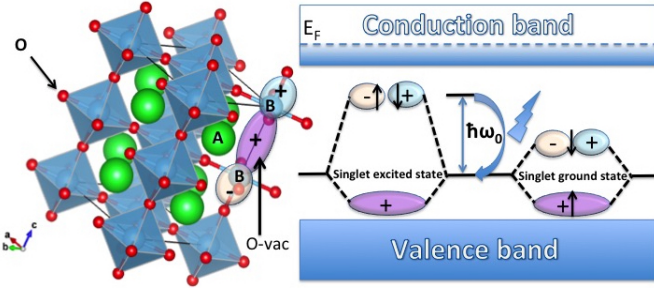


Figure 2. Left: crystal structure of  $ABO_3$  perovskites with an oxygen vacancy. Each vacancy traps two electrons in a singlet that fill up the bonding and anti-bonding molecular orbitals that result from the hybridization between the  $e_g$  wavefunctions of the two neighbouring B-ions. Right: schematic band structure of  $ABO_3$  perovskites with O vacancy impurity states. Spontaneous emission of in-gap color centers in such correlated metals occurs when the singlet excited state relaxes to the singlet ground state by emitting light in the visible.

charge  $e$ , the dielectric constant in free space  $\epsilon_0$ , the electronic density in the metal  $n$ , of the effective mass  $m^*$ ), while keeping the electrical conductivity  $\sigma = e^2\tau(n/m^*)$  (with  $\tau$  the scattering time) large enough by a judicious choice of the ratio  $n/m^*$ . The traditional strategy to adjust the ratio  $n/m^*$  relies on a trade-off between increasing  $n$ , as in wide-bandgap semiconductors, and/or decreasing  $m^*$  via heavy doping, as in the case of tin-doped indium oxide (ITO). Nevertheless, although ITO exhibits the largest conductivity for materials of its class (horizontal dashed line in Fig. 1), it is still much smaller than the conductivities of transition metals oxides, such as  $SrVO_3$  and  $CaVO_3$ . These materials have very good transmission efficiency of the order of 80%, except in the blue region [30], besides being excellent conductors (see Fig. 1), remarkable properties on which we capitalize to achieve enhanced and controllable spontaneous emission.

In what follows we propose for the first time an alternative physical mechanism, based on electronic correlations, for: i) reducing the plasmon frequency of transition metal oxides, making them transparent in the visible; and ii) controlling and enhancing the spontaneous emission of visible light. We start by recalling that moderate to strong electronic correlations, represented by the Hubbard interaction  $U$ , renormalizes the effective mass of carriers according to  $m^*(U)/m^*(0) = 1/[1 - (U/U_c)^2]$ , where  $U_c \approx 5\text{eV}$  is the critical value for the metal-to-Mott-insulator transition in these systems [32]. The plasmon frequency then modifies as

$$\omega_{pl}^2(U) = \omega_{pl}^2(0) \left[ 1 - (U/U_c)^2 \right]. \quad (1)$$

Such renormalization has indeed been observed in  $SrVO_3$  by ARPES [33], where  $U \approx 3.2\text{eV}$ , and  $\hbar\omega_{pl}(U) < 1.33\text{eV}$ , *i.e.* below the lower visible edge [30], see Fig. 1.

Having established the transparency of our material platform, in the following we specify the properties of the two-level quantum emitter. The crystal structure of  $ABO_3$  perovskites consists of corner shared  $BO_6$  octahedra, with the

transition metal B, inside each octahedron, and with the cation A, at the center of a unit cell of coordination 12 (Fig. 2). The removal of one oxygen atom from the structure, *i.e.* the introduction of an oxygen vacancy (O-vac), causes the trapping of two electrons, at the vacancy, each coming from a nearby B-ion. This scenario is consistent with LDA+DMFT calculations on oxygen deficient supercells in  $SrVO_3$ , and has been confirmed by ARPES for the case of UV irradiated  $SrVO_3$  crystals [34]. The large Coulomb repulsion imposes that the spins of these electrons be anti-parallel due to virtual tunneling processes. As a result, the ground state of an O-vac is a neutral, nonmagnetic spin-single state (an F color center), where the two electrons fill up the two molecular orbitals (bonding and anti-bonding) obtained from the hybridization of the original  $e_g$  orbitals of the neighboring B ions, Fig. 2.

The electronic structure at the O-vac discussed above can be calculated by the following two-site Hamiltonian

$$H = \sum_{i=1,2} \sum_{\sigma=\uparrow,\downarrow} \mathcal{E}_0 n_{i,\sigma} - t \sum_{\sigma=\uparrow,\downarrow} (c_{1,\sigma}^\dagger c_{2,\sigma} + h.c.) \\ + U \sum_{i=1,2} \sum_{\sigma=\uparrow,\downarrow} n_{i,\sigma} n_{i,-\sigma} + V \sum_{\sigma,\sigma'} n_{1,\sigma} n_{2,\sigma'},$$

where  $\mathcal{E}_0$  is the onsite energy,  $t$  is the direct tunnelling,  $U$  is the onsite Coulomb repulsion that opposes double occupancy,  $V$  is the nearest neighbour Coulomb repulsion that opposes direct tunneling, and  $n_{i,\sigma} = c_{i,\sigma}^\dagger c_{i,\sigma}$  with  $c_{i,\sigma}^\dagger$  and  $c_{i,\sigma}$  corresponding to the creation and annihilation operators for the electrons at the two B-ion,  $d$ -orbitals. A mean field treatment of the Coulomb interactions allows us to replace  $\sum_{\sigma=\uparrow,\downarrow} [\mathcal{E}_0 n_{i,\sigma} + U n_{i,\sigma} n_{i,-\sigma}]$  by  $\sum_{\sigma=\uparrow,\downarrow} \mathcal{E}_{i,\sigma} n_{i,\sigma}$ , in terms of  $\mathcal{E}_{i,\sigma} = \mathcal{E}_0 + U \langle n_{i,-\sigma} \rangle$ , and also to replace  $\sum_{\sigma,\sigma'} [t \delta_{\sigma,\sigma'} c_{1,\sigma}^\dagger c_{2,\sigma'} - V n_{1,\sigma} n_{2,\sigma'}]$  by  $\sum_{\sigma=\uparrow,\downarrow} \mathcal{T}_\sigma c_{1,\sigma}^\dagger c_{2,\sigma}$ , in terms of  $\mathcal{T}_\sigma = t - V \sum_{\sigma'} \langle c_{1,\sigma} c_{2,\sigma'}^\dagger \rangle$ . The Hamiltonian is now quadratic and can be diagonalized providing eigenvalues

$$E_\sigma^\pm = \frac{\mathcal{E}_{1,\sigma} + \mathcal{E}_{2,\sigma} \pm \sqrt{(\mathcal{E}_{1,\sigma} - \mathcal{E}_{2,\sigma})^2 + 4\mathcal{T}_\sigma^2}}{2}. \quad (2)$$

The Hilbert space for the O-vac problem is spanned by four basis states  $|1, \uparrow\downarrow; 2, 0\rangle, |1, \uparrow; 2, \downarrow\rangle, |1, \downarrow; 2, \uparrow\rangle, |1, 0; 2, \uparrow\downarrow\rangle$ , in terms of which  $\langle n_{i,-\sigma} \rangle$  and  $\langle c_{1,\sigma} c_{2,\sigma'}^\dagger \rangle$  must be calculated. If the two electrons occupy the same molecular orbital,  $\langle n_{i,-\sigma} \rangle = 1/2$  (projected subspace of doubly-occupied states), whereas if the two electrons occupy a different molecular orbital each,  $\langle n_{i,-\sigma} \rangle = 0$  (projected subspace of singly-occupied states). Analogously,  $\langle c_{1,\sigma} c_{2,\sigma'}^\dagger \rangle = \delta_{\sigma,\sigma'}/2$  (projected subspace of mixed singly- and double-occupied states). For  $U > 2(2t - V)$  the ground state  $|g\rangle$ , corresponds to a singlet configuration with the two electrons occupying a different molecular orbital each. There is a low lying singlet excited state  $|le\rangle$ , corresponding to a doubly-occupied bonding orbital, and a high energy singlet excited state  $|he\rangle$ , corresponding to a doubly-occupied anti-bonding orbital. The  $|g\rangle$  and  $|he\rangle$  states are shown in Fig. 2 and their splitting is

$$\hbar\omega_0 = 2t - V + \frac{U}{2}. \quad (3)$$

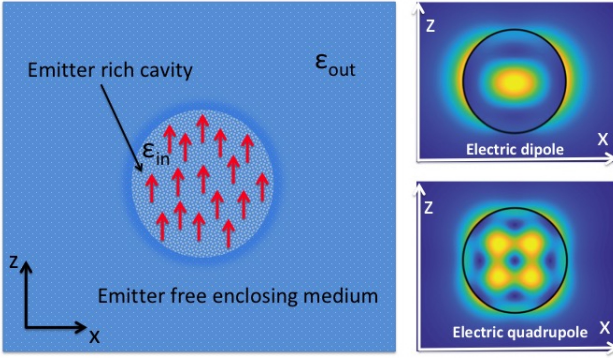


Figure 3. Left: Oxygen vacancy rich, spherical cavity of dielectric constant  $\epsilon_{in}$ , containing an agglomerate of electric dipoles (red arrows), inside an otherwise O-vac free enclosing host of dielectric constant  $\epsilon_{out}$ . Right: normal electromagnetic modes inside the cavity according to Mie's theory; only the electric dipole (top) and quadrupole (bottom) modes are shown for clarity.

By using typical values for the hopping,  $t \approx 1.0\text{eV}$ , and Hubbard parameters,  $U \approx 3.2\text{eV}$ , and  $V \approx 0.8\text{eV}$ , consistent with GW+DMFT and LDA+DMFT calculations for  $\text{SrVO}_3$  [35], we obtain  $\hbar\omega_0 \approx 2.8\text{eV}$  for the characteristic emitter's energy, which corresponds to light emission/absorption in the blue, exactly where  $\text{SrVO}_3$  transmits poorly [30]. Similar values for  $\hbar\omega_0$  can also be found for other  $\text{ABO}_3$  Perovskites, using similar values for  $t, U, V$ , satisfying  $V < t < U$ , all within the visible, as observed in photoluminescence experiments in a variety of disordered Perovskites such as  $\text{BaTiO}_3$ ,  $\text{CaTiO}_3$ ,  $\text{PbTiO}_3$ ,  $\text{LiNbO}_3$ ,  $\text{SrWO}_4$ , besides  $\text{SrVO}_3$  itself [37].

We are now ready to calculate the spontaneous emission rate  $\Gamma$  for a dilute and homogeneous collection of O-vac impurity states embedded in a correlated metal whose optical

properties depend on the correlation strength  $U$  through the dielectric function  $\epsilon(\omega, U) = \epsilon_0 \epsilon_r(\omega, U)$ . To this end we calculate the electric-dipole matrix element between the singlet, ground  $|g\rangle$ , and highest excited  $|he\rangle$  states

$$|\langle g | H_{int} | he \rangle| = \sqrt{\frac{\hbar\omega_0}{2\epsilon_0 \epsilon_r(\omega_0, U) V}} \hat{\epsilon}_\lambda \cdot \langle g | \vec{\mu} | he \rangle, \quad (4)$$

describing the coupling between an O-vacancy, with nonzero electric-dipole moment  $\vec{\mu}$  between the bonding and anti-bonding orbitals, and radiation with polarization  $\hat{\epsilon}_\lambda$ . Here  $V$  is the volume and  $\epsilon_r(\omega, U) = \epsilon_1(\omega, U) + i\epsilon_2(\omega, U)$ , with

$$\begin{aligned} \epsilon_1(\omega, U) &= 1 - \frac{\omega_{pl}^2(U)}{\omega^2 + \gamma^2}, \\ \epsilon_2(\omega, U) &= \frac{\gamma\omega_{pl}^2(U)}{\omega(\omega^2 + \gamma^2)}, \end{aligned} \quad (5)$$

is the relative permittivity of a lossy,  $\gamma \neq 0$ , medium. For isotropic systems with electric dipole moment  $\vec{\mu} = \mu\hat{z}$ , we can write  $|\hat{\epsilon}_\lambda \cdot \langle g | \vec{\mu} | he \rangle|^2 = \mu^2 |\langle \hat{\epsilon}_\lambda \cdot \hat{z} \rangle|^2 = \mu^2/3$ . By defining the quantity  $g^2 = \hbar\omega_0 \mu^2 / 6\epsilon_0$ , and recalling the definition of the spectral distribution of electromagnetic modes in the medium,  $\mathcal{A}_U(\omega, |\mathbf{k}|) = -(2c|\mathbf{k}|/\pi) \mathcal{I}m[G_U^R(\omega, \mathbf{k})]$ , where retarded photon propagator is [38]

$$G_U^R(\omega, \mathbf{k}) = \frac{1}{\epsilon_1(\omega, U)\omega^2 - c^2|\mathbf{k}|^2 + i\epsilon_2(\omega, U)\omega^2}, \quad (6)$$

we can use Fermi's golden rule to calculate the spontaneous emission rate for the  $i$ -th isolated, single O-vac, in terms of the value in free space,  $\Gamma_0 = (2\pi/\hbar^2)g^2[\omega_0^2/\pi^2 c^3]$ , as

$$\Gamma_i(U) = \left(\frac{2\pi}{\hbar^2}\right) \left[\frac{g^2}{\epsilon_r(\omega_0, U)}\right] \int_0^\infty \frac{dk}{\pi^2} k^2 \left\{ \frac{2ck\epsilon_2(\omega, U)\omega^2}{[\epsilon_1(\omega, U)\omega^2 - c^2k^2]^2 + \epsilon_2^2(\omega, U)\omega^4} \right\} = \eta(\omega_0, U)\Gamma_0. \quad (7)$$

This result generalizes the one obtained for the decay rate of excited atoms in absorbing dielectric insulators [39], to the case of correlated metallic systems. The real,  $\epsilon_1(\omega_0, U) = \eta^2(\omega_0, U) - \kappa^2(\omega_0, U)$ , and imaginary,  $\epsilon_2(\omega_0, U) = 2\eta(\omega_0, U)\kappa(\omega_0, U)$ , parts of the relative permittivity are given in terms of the refraction index,  $\eta(\omega, U)$ , and extinction coefficient,  $\kappa(\omega, U)$ , of the correlated metal. The integral over  $k$  was done by extending the integration from  $[0, \infty)$  to  $(-\infty, \infty)$ , and closing the contour of integration in the upper-half of the complex  $k$  plane. Note that, since  $\eta(\omega_0, U) < 1$  inside the metal, the spontaneous emission rate  $\Gamma_i$  for the  $i$ -th isolated O-vac is smaller than the result in free space  $\Gamma_0$  and the role of  $\eta(\omega_0, U) \neq 0$ , which encodes electronic correlations, is to allow for transmission in the visible, forbidden for  $\omega_0 < \omega_{pl}(0)$ , *i.e.*, in the absence of correlations.

The highly diffusive character of O-vacs in oxides, which naturally occur even in the purest  $\text{ABO}_3$  samples, allows for their migration and easy accumulation near grain boundaries [40], their binding to foreign dopants [41], or their segregation at other defects [42]. Alternatively, O-vac rich regions can be engineered in a controlled way via microwave irradiation [43] or pulsed laser deposition [44], forming thermodynamically stable agglomerates of micrometer sizes containing a large number of color centers. In order to model such agglomerates we consider a collection of electric-dipoles,  $\vec{\mu}$ , enclosed by a spherical cavity of radius  $a$ , which acts as a boundary between a region rich in O-vacs and the bulk metal, Fig. 3. The local fields on a given dipole, due to the presence of all other dipoles, is accounted for by the usual Lorentz local-field factor,  $\mathcal{L}_{cav} = |(\epsilon(\omega_0) + 2)/3|$  [45]. Most importantly, spon-

taneous emission will now occur due to the coupling to the cavity's electromagnetic modes. The dipole-rich region can be seen as an inclusion, characterized by a dielectric constant,  $\varepsilon_{in}$ , and the enclosing metal as a host, with dielectric constant,  $\varepsilon_{out}$ . The mismatch  $\varepsilon_{in} \neq \varepsilon_{out}$ , allows for the reflection of the emitted radiation back into the center of the cavity, transforming the dipole-rich region into a Mie resonator. In this case, the SE rate corresponds to the convolution [46]

$$\Gamma_{cav} = \Gamma_0 \int_0^\infty d\omega F_{cav}(\omega) \left| \frac{\varepsilon_{in}(\omega) + 2}{3} \right|^2 \eta_{in}(\omega) \delta(\omega - \omega_0), \quad (8)$$

where the Purcell cavity-enhancement factor  $F_{cav}(\omega)$  is [47]

$$F_{cav}(\omega) = \frac{3\pi c^3}{\omega} \sum_{q=1}^{\infty} \text{Im} \left[ \frac{1}{V_{1,0,q} \omega_{1,0,q} (\omega_{1,0,q} - \omega)} \right], \quad (9)$$

and  $V_{j,m_z,q}$  are the mode volumes for the  $(j, m_z, q)$  cavity modes corresponding to the complex valued eigenfrequencies  $\omega_{j,m_z,q} = \omega'_{j,m_z,q} + i\omega''_{j,m_z,q}$ . For dipoles along the  $\hat{z}$  direction only the  $j = 1$  and  $m_z = 0$  contributions are relevant and the associated frequencies are solutions to the equation

$$\sqrt{\varepsilon_{in}} \psi_1(k_{in}a) \xi_1'(k_{out}a) - \sqrt{\varepsilon_{out}} \psi_1'(k_{in}a) \xi_1(k_{out}a) = 0, \quad (10)$$

where  $k_{in,out} = \omega/c_{in,out}$ , with  $c_{in,out}$  being the speed of light inside and outside the cavity, and  $\psi_1(x) = xj_1(x)$  and  $\xi_1 = xh_1^{(1)}(x)$ , are written in terms of the  $j_1(x)$  spherical Bessel function and the  $h_1^{(1)} = j_1(x) + iy_1(x)$  spherical Hankel function, with the prime indicating derivative with respect to its argument. The mode volumes,  $V_{1,0,q}$ , need not be identical to the physical cavity volume,  $V_{cav} = 4\pi a^3/3$ , and, in fact, are a decreasing function of  $q$  [47]. The cavity modes are, in turn, characterized by a discrete set of frequencies,  $\omega'_{1,0,q}$ , that increase with  $q = 1, 2, \dots$ , and inverse lifetimes,  $\omega''_{1,0,q}$ , that decrease with  $q = 1, 2, \dots$  [47].

In Fig. 4 the normalized SE rate  $\Gamma/\Gamma_0$  is shown, as a function of  $\omega_0/\omega_{pl}$  (left) and of  $U/U_c$  (right) for: i) a single emitter in a nearly lossless transparent metal (red dashed line); and ii) an agglomerate of emitters confined to an O-vac rich spherical cavity, regarded as an optically active inclusion in an otherwise transparent metallic host (solid blue line). The case of SrVO<sub>3</sub>, with  $U \approx 3.2\text{eV}$ ,  $\hbar\omega_{pl} < 1.33\text{eV}$  and  $\hbar\omega_0 \approx 2.8\text{eV}$ , is represented by black arrows at  $\omega_0/\omega_{pl} = 2.2$  (left) and  $U/U_c = 0.67$  (right). The real part of the cavity frequencies,  $\omega'_{1,0,q}$ , are determined by the ratios: i)  $\varepsilon_{in}/\varepsilon_{out} \neq 1$ ; and ii)  $k_{in}a \sim 1$ . If the emitter's frequency,  $\omega_0$ , coincides with one of the cavity modes' frequencies,  $\omega'_{1,0,q}$ , i.e., if they are *on-resonance*, then spontaneous emission can be strongly enhanced. On the other hand, if the emitter and the cavity modes are *off-resonance*, then spontaneous emission is strongly suppressed to values even smaller than half the one in free space, see Fig. 4. If we recall that  $\omega_0(t, V, U)$  and  $\omega_{pl}(U)$  are functions of  $t, V$  and  $U$ , it is clear that, even the smallest variations in any of such parameters, especially  $U$ , could switch the on- and off- resonance situations, causing the emitter to blink in a controlled way.

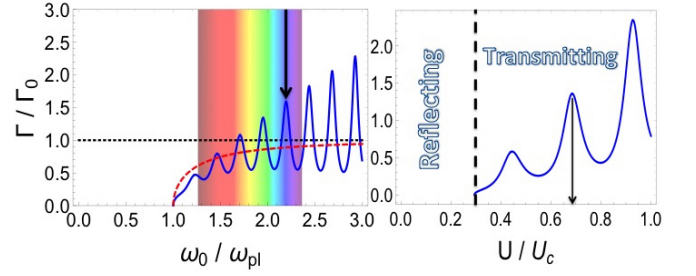


Figure 4. Left: spontaneous emission rate,  $\Gamma/\Gamma_0$ , as a function of the emitter's frequency,  $\omega_0/\omega_{pl}$ . Black arrows at  $\omega_0 = 2.2\omega_{pl}$  and  $U/U_c = 0.67$  correspond to SrVO<sub>3</sub>. The red (dashed) line is for dilute, isolated emitters in a nearly lossless metal, and the full (blue) line is for a resonant spherical cavity, filled up with an agglomerate of emitters, again in a nearly lossless metal. Right: the normalized SE rate as a function of the correlation strength,  $U$ , relative to the critical value,  $U_c$ , for the Mott insulator transition. For values of  $U$  corresponding to the situation of *on-resonance* the SE rate,  $\Gamma$ , rapidly and significantly increases with respect to the free space value,  $\Gamma_0$ .

A number of strategies are known to dynamically vary the values of the parameters  $t, V$  and  $U$ , thus allowing for the tuning of the resonances in a controlled way. For instance, the Hubbard  $U$  parameter can be decreased by almost 10% on femtosecond timescales via laser driving in correlated materials [48]. Dynamically decreasing  $U$  would not only red-shift the emitter's frequency  $\omega_0(t, V, U)$ , but would, at the same time, blue-shift the plasmon frequency  $\omega_{pl}(U)$ , producing, simultaneously, an off-resonance situation while reducing the refraction index of the material,  $\eta(U) \rightarrow 0$ . Alternatively, with  $U$  fixed one could also use mechanical strain, normal,  $\varepsilon_{ij}$ , or shear,  $\gamma_{ij}$ , with  $i, j = x, y, z$ , to control spontaneous emission. In ABO<sub>3</sub> oxides strain can be used to modify both the B-O-B and B-B bond angles, through the rotation of the oxygen octahedra [49], which leads to changes in the hopping parameter  $t$  and positions of the  $e_g$  levels. In this case, although the plasmon,  $\omega_{pl}$ , and cavity mode,  $\omega_{1,0,q}$ , frequencies are kept unchanged, the emitter's frequency,  $\omega_0(t, V, U)$ , can be tuned via strain, which modifies  $t(\varepsilon_{ij}, \gamma_{ij})$ .

In conclusion, we have investigated spontaneous emission in transparent metals subject to electronic correlations. We have demonstrated that there exists a critical value for the correlation strength  $U$ , above which spontaneous emission is not only allowed but is also strongly enhanced due to resonant coupling between the emitter's electric dipole moment to long-lived electromagnetic modes inside an optically cavity filled up with two-level color centers (oxygen vacancies agglomerates). The situations *on- and off- resonance* can be tuned in a controlled way either through variations of the correlation strength and/or by applying mechanical strain/stress, thus strongly enhancing or suppressing spontaneous emission. Altogether, our results suggest concrete and feasible routes towards the external control of spontaneous emission in metallic systems that may be applied to solid state single photon sources to produce photons on demand.

We acknowledge CNPq, CAPES, and FAPERJ for financial support. F.A.P. also thanks the The Royal Society-Newton Advanced Fellowship (Grant no. NA150208) for financial support.

- 
- [1] M. Lipson, *Journal of Lightwave Technology* **23**, 4222 (2005).
- [2] P. Lodahl, S. Mahmoodian, and S. Stobbe, *Rev. Mod. Phys.* **87**, 347 (2015).
- [3] E. M. Purcell, *Phys. Rev.* **69**, 681 (1946).
- [4] A. Goban, C.-L. Hung, S.-P. Yu, J.D. Hood, J.A. Muniz, J.H. Lee, M.J. Martin, A.C. McClung, K.S. Choi, D.E. Chang, O. Painter, and H.J. Kimble, *Nature Commun.* **5**, 3808 (2014).
- [5] Peter, E.; Senellart, P.; Martrou, D.; Lemaitre, A.; Hours, J.; Gerard, J. M.; Bloch, J. Exciton-Photon Strong-Coupling Regime for a Single Quantum Dot Embedded in a Microcavity. *Phys. Rev. Lett.* **95**, 067401(2005).
- [6] M. Arcari, I. S. Ilnier, A. Javadi, S. Lindskov Hansen, S. Mahmoodian, J. Liu, H. Thyrrerstrup, E.H. Lee, J.D. Song, S. Stobbe, and P. Lodahl, *Phys. Rev. Lett.* **113**, 093603 (2014).
- [7] K. J. Tielrooij *et al.*, *Nature Physics* **11**, 281 (2015).
- [8] W. J. M. Kort-Kamp, B. Amorim, G. Bastos, F. A. Pinheiro, F. S. S. Rosa, N. M. R. Peres, and C. Farina *Phys. Rev. B* **92**, 205415 (2015).
- [9] Regmi, R.; Berthelot, J.; Winkler, P. M.; Mivelle, M.; Proust, J.; Bedu, F.; Ozerov, I.; Begou, T.; Lumeau, J.; Rigneault, *Nano Lett.* **16**, 5143 (2016).
- [10] Tanaka, K.; Plum, E.; Ou, J. Y.; Uchino, T.; Zheludev, N. I., *Phys. Rev. Lett.* **105**, 227403 (2010).
- [11] Muskens, O. L.; Giannini, V.; Sanchez-Gil, J. A.; Gómez Rivas, *Nano Lett.* **7**, 2871 (2007).
- [12] M. A. Noginov, H. Li, Yu. A. Barnakov, D. Dryden, G. Nataraj, G. Zhu, C. E. Bonner, M. Mayy, Z. Jacob, and E. E. Narimanov, *Opt. Lett.* **35**, 1863 (2010).
- [13] D. J. Roth, A. V. Krasavin, A. Wade, W. Dickson, A. Murphy, S. K'ena-Cohen, R. Pollard, G. A. Wurtz, D. Richards, S. A. Maier, and A. V. Zayats *ACS Photonics* **4** 2513 (2017).
- [14] S. Liu *et al.* *Nano Letters* **18**, 6906 (2018).
- [15] J. Bohn, T. Bucher, K. E. Chong, A. Komar, D.-Y. Choi, D. N. Neshev, Y. S. Kivshar, T. Pertsch, and I. Staude *Nano Letters* **18**, 3461 (2018).
- [16] W. J. M. Kort-Kamp, F. S. S. Rosa, F. A. Pinheiro, and C. Farina *Phys. Rev. A* **87**, 023837 (2013).
- [17] M. Pelton, *Nature Photonics* **9**, 427 (2015).
- [18] M. Makarova, Y. Gong, S.-L. Cheng, Y. Nishi, S. Yerci, R. Li, L. Dal Negro, and J. Vuckovic, *IEEE Journal of Selected Topics in Quantum Electronics* **16**, 132 (2010).
- [19] Arruda T.J., Martinez A.S., Pinheiro F.A., Bachelard R., Slama S., Courteille P.W. *Fano Resonances in Plasmonic Core-Shell Particles and the Purcell Effect*. In: Kamenetskii E., Sadreev A., Miroshnichenko A. (eds) *Fano Resonances in Optics and Microwaves*. Springer Series in Optical Sciences, **219** Springer, Cham (2018).
- [20] T.J. Arruda, R. Bachelard, J. Weiner, S. Slama, PhW Courteille, Fano resonances and fluorescence enhancement of a dipole emitter near a plasmonic nanoshell. *Phys. Rev. A* **96**, 043869 (2017).
- [21] N. de Sousa, J. J. Sáenz, A. García-Martín, L. S. Froufe-Pérez, and M. I. Marqués, *Phys. Rev. A* **89**, 063830 (2014).
- [22] N. de Sousa, J. J. Sáenz, F. Scheffold, A. García-Martín, and L. S. Froufe-Pérez, *Phys. Rev. A* **94**, 043832 (2016).
- [23] D. Szilard, W. J. M. Kort-Kamp, F. S. S. Rosa, F. A. Pinheiro, and C. Farina, *Phys. Rev. B* **94**, 134204 (2016).
- [24] V. Krachmalnicoff, E. Castanié, Y. De Wilde, and R. Carminati, *Phys. Rev. Lett.* **105**, 183901 (2010).
- [25] M. B. Silva Neto, D. Szilard, F. S. S. Rosa, C. Farina, and F. A. Pinheiro *Phys. Rev. B* **96**, 235143 (2017).
- [26] W. Moerner and M. Orrit, *Science* **283**, 1670 (1999).
- [27] B. O'regan and M. Gratzel, *Nature (London)* **353**, 737 (1991).
- [28] R. A. L. Vallée, M. Van der Auweraer, W. Paul, and K. Binder, *Phys. Rev. Lett.* **97**, 217801 (2006).
- [29] P. Michler *et al.*, *Science* **290**, 2282 (2000).
- [30] L. Zhang *et al.* *Nature Materials* **15**, 204 (2016).
- [31] X. Yu, T. J. Marks, A. Facchetti, *Nature Materials* **15**, 383 (2016).
- [32] M. C. Gutzwiller, *Phys. Rev. A* **137**, A1726 (1965); W. F. Brinkmann and T. M. Rice, *Phys. Rev. B* **2** 4302 (1970).
- [33] T. Yoshida, K. Tanaka, H. Yagi, A. Ino, H. Eisaki, A. Fujimori, and Z.-X. Shen, *Phys. Rev. Lett.* **95**, 146404 (2005).
- [34] S. Backes, *et al.*, *Phys. Rev. B*, **94**, 241110(R) (2016).
- [35] C. Taranto, *et al.*, *Phys. Rev. B* **88**, 165119 (2013).
- [36] Y. Aiura, F. Iga, Y. Nishihara, H. Ohnuki, and H. Kato, *Phys. Rev. B* **47**, 6732 (1993).
- [37] P. S. Pizani, *et al.*, *Appl. Phys. Lett.* **81**, 253 (2002).
- [38] A. A. Abrikosov, L. P. Gorkov, and I. E. Dzyaloshinski, *Methods of Quantum Field Theory in Statistical Physics*, Dover Publications Inc., New York (1975).
- [39] S. M. Barnett, B. Huttner, R. Loudon, and R. Matloob, *J. Phys. B: At. Mol. Opt. Phys.* **29**, 3763 (1996).
- [40] M. Schie, A. Marchewka, T. Müller, R. A. De Souza, and R. Waser, *J. Phys: Condens. Matter* **24**, 485002 (2012).
- [41] G Arora and D S. Aidhy, *Journal of Materials Chemistry A* **5**, 4026 (2017).
- [42] B. J. Nyman, E. E. Helgee, and G. Wahnström, *Appl. Phys. Lett.* **100**, 061903 (2012).
- [43] G. L. Kabongo, T. N. Y. Khawula, T. Thokozani, E. G. Nyongombe, K. Ozoemena and S. Dhlamini, *Journal of Nanosciences: Current Research* **3**, 1000125 (2018).
- [44] F. V. E. Hensling, D. J. Keeble, J. Zhu, S. Brose, C. Xu, F. Gunkel, S. Danylyuk, S. S. Nonnenmann, W. Egger, and R. Dittmann, *Scientific Reports* **8**, 8846 (2018).
- [45] H. Lorentz, *The Theory of Electrons and Its Application to the Phenomena of Light & Radiant Heat*, 2nd Edition, Dover Publications, New York (1915).
- [46] S. Haroche and D. Kleppner, *Cavity Quantum Electrodynamics*, *Phys. Today* **42**, 24 (1989).
- [47] X. Zambrana-Puyalto and N. Bonod, *Phys. Rev. B* **91**, 195422 (2015).
- [48] N. T.-Dejean, M. A. Sentef, and A. Rubio, *Phys. Rev. Lett.* **121**, 097402 (2018).
- [49] W. Lu, W. Song, P. Yang, J. Ding, G. M. Chow and J. Chen, *Scientific Reports* **5**, 10245 (2015).